Plant Mol Biol Rep
DOI 10.1007/s11105-009-0148-6

Analysis of RPS15aE, an Isoform of a Plant-Specific Evolutionarily Distinct Ribosomal Protein in *Arabidopsis thaliana*, Reveals its Potential Role as a Growth Regulator

Kathleen Szick-Miranda · Ammar S. Zanial · Ali S. Zanial · Stacey Abidayo · Karie L. C. Slater

Abstract There is increasing evidence for ribosome heterogeneity in biological systems. In *Arabidopsis thaliana*, the ribosomal protein S15a is encoded by six separate genes, which fall into two evolutionarily distinct categories (Type I and Type II). Type I S15a is a universally conserved component of cytosolic ribosomes, whereas there is ambiguity as to the specific subcellular location of Type II S15a (cytosolic and/or mitochondrial ribosomes). In this study, we investigated the functional significance of the distinct form of ribosomal protein S15a (Type II) in *Arabidopsis* by examining: the evolutionary relationship of eukaryotic S15a proteins with respect to organellar homologs, the expression of individual Type II S15a genes during various developmental stages by RT-PCR, and the phenotypes of an insertional mutation into the *RPS15aE* gene. The Type II S15a proteins are plant specific, and the duplication event that gave rise to the Type II S15a genes appears to have occurred during the evolution of land plants. The genes encoding Type II S15a in *Arabidopsis* are differentially expressed, and mutant plants in which the gene encoding S15aE is knocked down produce larger leaves, longer roots, and possess larger cells than wild-type plants suggesting that the RPS15aE isoform of Type II S15a may act as a regulator of translational activity. Our results add significantly to the understanding of the protein constitution of plant ribosomes and the functional significance of ribosome heterogeneity.

Electronic supplementary material The online version of this article (doi:10.1007/s11105-009-0148-6) contains supplementary material, which is available to authorized users.

K. Szick-Miranda (✉) · A. S. Zanial · A. S. Zanial · S. Abidayo · K. L. C. Slater
Department of Biology, California State University, Bakersfield, CA 93311, USA
e-mail: kszick-miranda@csub.edu

Keywords *Arabidopsis* · Ribosome · Ribosomal protein · Protein synthesis · Translational regulation

Introduction

Protein synthesis is an absolute requirement for plant growth and development. It is a complex, multistep process that involves ribosomes; initiation, elongation, and release factors; aminoacyl tRNAs; and mRNA (Nygård and Nilsson 1990; Hershey 1991; Merrick and Hershey 1996; Proud 2007). Ribosomes, which catalyze protein synthesis, are complex macromolecules composed of three or four distinct rRNAs and up to 80 proteins. The structure and function of both prokaryotic and eukaryotic ribosomes have been investigated with the prokaryotic emphasis on the ribosomes of *Escherichia coli* and the eukaryotic emphasis on ribosomes of Baker's yeast (*Saccharomyces cerevisiae*) and rat (*Rattus rattus* and *Rattus norvegicus*). Three-dimensional visualization from crystallographic data have added significantly to the knowledge of eukarytoic ribosome structure (Verschoor et al. 1996; Spahn et al. 2001, 2004; Manuell et al. 2005; Chandramouli et al. 2008), whereas proteomic analyses have contributed to the knowledge of eukaryotic ribosomal protein (r-protein) composition and posttranslational modifications (Louie et al. 1996; Lee et al. 2002; Odintsova et al. 2003; Chang et al. 2005; Giavalisco et al. 2005; Manuell et al. 2005; Yu et al. 2005; Carroll et al. 2008).

Early studies indicated that plant cytosolic ribosomes were slightly smaller than their mammalian counterparts (Cammarano et al. 1972; Verschoor et al. 1996); however, recent advances in genomics and proteomics have allowed for a more detailed understanding of higher plant ribosomes specifically those of *Arabidopsis thaliana* (Barakat et al. 2001; Chang et al. 2005; Giavalisco et al. 2005; Carroll et

Published online: 26 September 2009

al. 2008). Notably, combined proteomic analyses are indicative of ribosome heterogeneity due to expression of specific genes as well as posttranslational modifications.

Eukaryotic r-protein S15a is orthologous to S8 of eubacteria (Wool et al. 1995; Tishchenko et al. 2001). Eubacterial S8 binds 16S rRNA in the 30S subunit and is considered crucial for ribosome assembly (Held et al. 1974; Svensson et al. 1988; Brodersen et al. 2002). The N-terminal domain of S8 comprises a double-stranded DNA-binding motif present in several proteins including DNaseI, prokaryotic initiation factor 3 (IF3), and DNA methyltransferase (Davies et al. 1996). Also, S8 has been shown to act as a translational repressor by binding to the mRNA of its own operon (*spc*), which encodes ten ribosomal proteins (Dean et al. 1981). In eukaryotes, the over-expression of S15a in *Drosophila melanogaster* suppresses a yeast temperature-sensitive mutant defective in protein synthesis suggesting a role for S15a in translational initiation (Lavoie et al. 1994), whereas an S15a gene knockdown in zebrafish (*Danio rerio*) causes severely restricted brain development and growth, circulatory defects, and moderate tail development (Uechi et al. 2006). In addition, zebrafish that is heterozygous for a mutant S15a allele showed a significant increase in tumor formation suggesting that this protein may act as a tumor suppressor (Amsterdam et al. 2004).

In the *A. thaliana* genome, r-protein S15a is encoded by six genes (Barakat et al. 2001). The deduced polypeptide sequences of four genes (S15aA, C, D, and F) share a high-percent identity to the rat ortholog (between 73.1% and 77.7%), whereas the deduced polypeptide sequences for the additional two genes (S15aB and E) show a much lower-percent identity to rat S15a (47.6% and 48.8%, respectively; Chang et al. 2005). Utilizing various analyses, Chang et al. (2005) demonstrated that the deduced polypeptide sequences of the S15a genes fell into two evolutionarily distinct categories, Type I (S15aA, C, D, and F) and Type II (S15aB and E). Proteomic analyses of ribosomes from cultured *Arabidopsis* cells indicated that Type I is present in cytosolic ribosomes at amounts similar to the stoichiometry of the other ribosomal proteins, whereas Type II S15a may be present at substoichiometric levels (Chang et al. 2005). However, Adams et al. (2002) found that the product of the Type II gene, from *Arabidopsis* and tomato, can be imported into mitochondria in an *in vitro* system. The successful import of the Type II S15a gene product into mitochondria along with the absence of the *rps8* gene from the mitochondrion and nucleus of the angiosperms examined led Adams et al. (2002) to suggest that the Type II S15a gene product acts as a mitochondrial ribosomal protein. Lastly, in a recent proteomic analysis of *Arabidopsis* cytosolic ribosomes (Carroll et al. 2008), it was reported that the Type I S15a proteins are cytosolic r-proteins, whereas the Type II S15a proteins are mitochondrial r-proteins.

The goal of this study was to determine the functional significance of the Type II forms of S15a in *A. thaliana*. Towards this goal, we examine the evolutionary relationship of the Type I and Type II S15a proteins with respect to organellar S8 proteins. We also monitored the relative abundance of the two Type II S15a gene transcripts (*RPS15aB* and *RPS15aE*) during development. Lastly, we examined phenotypes of insertional mutations into the *RPS15aB* and *RPS15aE* genes. We demonstrate that the Type II S15a proteins are plant specific and that the *Arabidopsis* Type II S15a genes are differentially expressed. We also provide evidence that S15aE may act as a regulator of translational activity.

Materials and Methods

Plant Material and Growth Conditions

A. thaliana ecotype Columbia wild-type (WT) or transgenic seed were surface-sterilized for 5 min with 95% (*v*/*v*) ethanol followed by 5 min in 20% (*v*/*v*) bleach with 0.1% (*v*/*v*) Tween-20, rinsed three times in sterile water, and allowed to imbibe at 4°C. After 48 h, seeds were transferred to plates with solid Murashige and Skoog (MS; 1962) media (0.43% [*w*/*v*] MS salts [Sigma, St. Louis, MO], 0.8% [*w*/*v*] agar, 1% [*w*/*v*] sucrose, pH 5.7). Plates were placed in a growth chamber at 22°C under long-day photoperiod (16 h photoperiod, ~140 μmol m^{-2} s^{-1}). After 12 d, seedlings were transferred to soil. Seeds were germinated on MS media prior to transfer to soil to better assess early developmental stages for the phenotypic analysis described below. Plants were grown at 22°C under long-day photoperiod (16 h photoperiod, 200 μmol m^{-2} s^{-1}). Tissues harvested for RNA analyses were from 7-day seedlings or 5-week old plants. All tissues collected were flash frozen in liquid N_2 and ground with a mortar and pestle prior to nucleic acid extraction.

Arabidopsis T-DNA Insertion Lines

Arabidopsis T-DNA insertion lines were obtained from the *Arabidopsis* Biological Resource Center (Ohio State University; Alonso et al. 2003). Two hemizygous lines with putative insertions in *RPS15aB* (SALK_074808) or *RPS15aE* (SALK_118515) were made homozygous by successive self-crossing. Genotypes (WT, *rps15aB-mut1*, and *rps15aE-mut1*) were confirmed by conducting a combination of polymerase chain reactions (PCRs) with genomic DNA isolated from ABRC lines using gene-specific and T-DNA-specific primers. Primers designed to flank the T-DNA insertion (Fig. 1) identified WT and heterozygous plants, whereas gene-specific primers and a

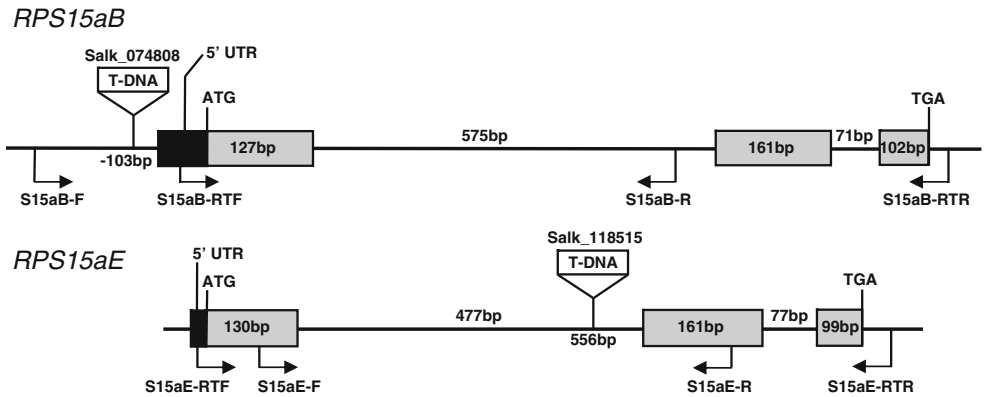

Fig. 1 Structure and organization of the Type II *S15a* genes. Schematic representation of Type II *RPS15a* open reading frames, introns, exons, 5′, and 3′ UTRs. Exons are represented as *shaded boxes* and introns are represented by *lines drawn between exons*. Translation start (*ATG*) and termination codons (*TGA*) are indicated. *Black shading* indicates putative length of the 5′UTR. The locations of *T-DNA* insertions are indicated. Numbers in exons and introns correspond to the length of the segment in base pairs. Positions of gene-specific primers are indicated by *arrows*; *F* forward primer and *R* reverse primer were utilized in PCR reactions, whereas *RT-F* forward primer and *RT-R* reverse primer were utilized in RT-PCR reactions

primer designed to bind to the left border (LB) of the T-DNA insert identified plants heterozygous or homozygous for the insert. Genomic DNA was isolated from approximately 100 mg of leaf tissue using the DNeasy Plant Mini kit (Qiagen, Valencia, CA) according to the manufacturer's protocol. PCRs were set up to produce a single amplicon with the gene-specific primer pair (F + R) or the gene-specific/T-DNA-specific primer pair (LB + R). The number of cycles and the annealing temperature used for each primer pair are indicated in Supplemental Table 1. Amplification products were resolved on a 0.8% (*w*/*v*) agarose gel stained with ethidium bromide. The PCR products obtained using the gene-specific/T-DNA-specific primer pair (LB + R) were purified with the QIAquick PCR Purification Kit (Qiagen, Valencia, CA) and sequenced (ICBR, University of Florida, Gainsville, FL) to determine the precise location of the T-DNA insertion.

RT-PCR Analysis

Total RNA was isolated from 100 mg of WT or homozygous mutant (*rps15aB-mut1* or *rps15aE-mut1*) frozen tissue using the RNeasy Plant Mini kit (Qiagen, Valencia, CA) according to the manufacturer's protocol with an on-column DNase digestion. Reverse transcriptase-polymerase chain reaction (RT-PCR) was performed with gene-specific primer pairs using 200 ng of total RNA utilizing the One-Step RT-PCR kit (Qiagen, Valencia, CA) according to the manufacturer's protocol. To confirm that the amplification was linear and to establish the number of amplification cycles for the detection of cDNA within the linear range, PCRs were carried out for *rps15aB*, *rps15aE*, and *rps6* for 20–35 cycles. Amplification products were resolved on 0.8% agarose gels stained with ethidium bromide. Primers designed to bind to *RPS6B* mRNA were utilized as an internal loading standard in separate reactions. The number of cycles and the annealing temperature used for each primer pair is indicated in Supplemental Table 1. The results shown are representative of three biological replicates.

Phenotypic Analysis

Fifteen plants each of WT and *rps15aE-mut1* were planted and observed daily. All plants were grown in controlled physiological conditions with 16 h photoperiod at ~120 μmol m^{-2} s^{-1} with an average temperature of 23°C. The plants were placed into pairs randomly (WT and *rps15aE-mut1*, for a total of 15 pairs) to minimize differences in the microenvironment. The number of days to reach each rosette leaf stage, budding, and flowering as well as the mass of the resultant seed was recorded for all 30 plants (15 WT, 15 *rps15aE-mut1*). At ten-, 12-, 14-rosette leaf stages, and at the time of the first-flower opening, the radius of the rosette (from the center of the rosette to the tip of the leaf) was measured for each of the 30 plants utilizing the largest leaf in the rosette. The same leaf was removed from the plant to measure the total leaf area using a leaf area meter (LI-3100, LI-COR, Lincoln, NE). The mean and the standard error of the mean were calculated for all parameters examined. The number of days to reach a developmental stage and the seed mass between WT and *rps15aE-mut1* was analyzed with a paired *t* test. Data from leaf radii and areas were analyzed using a two-way ANOVA with the following model; treatment (WT and *rps15aE-mut1*), size (radii and leaf areas at various developmental stages), replicates (15 total) as a random factor nested within

Table 1 Species utilized in evolutionary analyses

Species	Abbreviation	Common name	Accession number(s)[a]
Arabidopsis thaliana	*Ath*	*Arabidopsis*	P56801(chloroplast S8)
			At1g07770 (S15a Type I)
			At4g29430 (S15a Type II)
Chlamydomonas reinhardtii	*Cre*	Green algae	P59775 (chloroplast S8)
			XM_001700604 (S15a)
Chlorokybus atmophyticus	*Cat*	Green algae	ABD62254 (chloroplast S8)
			ABO15124 (mitochondrial S8)
Dictyostelium discoideum	*Ddi*	Slime mold	O21036 (mitochondrial S8)
Drosophila melanogaster	*Dme*	Fruit fly	Z21673 (S15a)
Haloarcula marismortui	*Hma*	Archaeon	X58395 (S8)
Methanococcus jannaschii	*Mja*	Archaeon	P54041 (S8)
Oryza sativa	*Osa*	Rice	P0C492 (chloroplast S8)
			AK119795 (S15a Type I)
			AK121591 (S15a Type II)
Ostreococcus tauri	*Ota*	Green algae	YP_717242 (chloroplast S8)
			YP_717271 (mitochondrial S8)
Physcomitrella patens	*Ppa*	Moss	AP005672 (chloroplast S8)
			XM_001763413 (S15a Type I)
Picea abies	*Pab*	Norway spruce	AJ001024 (chloroplast S8)
Picea sitchensis	*Psi*	Sitka pine	EF085371 (S15a Type I)
			EF082728 (S15a Type II)
Populus trichocarpa	*Ptr*	Poplar	A4GYU6 (chloroplast S8)
			EF145011 (S15a Type I)
			EF146122 (S15a Type II)
Saccharomyces cerevisiae	*Sce*	Baker's yeast	Q03799 (mitochondrial S8)
			X77688 (S15a)
Selaginella moellendorfii	*Smo*	Spikemoss	gnl|Selmo1|137784 (chloroplast S8)
			gnl|Selmo1|228163 (S15a Type I)
			gnl|Selmo1|432268 (S15a Type II)
Rattus norvegicus	*Rno*	Rat	NM053982 (S15a)

[a] All accession numbers correspond to sequences readily available in GenBank with the exception of *Selaginella* submissions, which are available at through the *Selaginella* Genomics Project (http://xselaginella.genomics.purdue.edu/)

treatment and all possible interactions. This was followed by a Tukey's post hoc analysis to test for significant differences (Minitab, Version 15.1.0.0, Minitab Inc., State College, PA). Root length was measured for individual WT and *rps15aE-mut1* seedlings grown on the same MS plate. The data were analyzed with a two-sample *t* test, and the mean and the standard error of the mean were calculated.

Microscopic Analyses

Roots were observed with a stereoscopic microscope (EZ4D, Leica Microsystems Inc., USA). Whole leaves and leaf cells were observed with an Olympus BH-2 BHTU Light Microscope (Olympus America Inc., USA). Palisade cells in the subepidermal layer from the center of the leaf blade, between the midvein and the leaf margin, were analyzed at the 14-leaf stage and at 6 weeks postimbibition. The mean cell area per leaf and standard error of the mean were calculated from the area of ten randomly chosen cells (Scion Image, MD, USA). Mean area between WT and *rps15aE-mut1* was analyzed with a paired *t* test.

Sequence Divergence and Phylogenetic Analyses

S15a and S8 homology searches were performed utilizing the BLASTP search algorithm against the nonredundant database at NCBI and the *Selaginella* Genomics Project 2009 (http://xselaginella.genomics.purdue.edu/). Amino acid sequence alignments were generated using ClustalW (Thompson et al. 1994) and optimized manually after visual inspection (alignment available upon request). Pairwise

uncorrected distances were calculated using PAUP test version 4.0b10 (PPC/Altivec; Sinauer Associates, Sunderland, MA). The aligned polypeptide sequences were subjected to maximum parsimony and neighbor-joining analyses (p-distances) using PAUP and Bayesian analyses using MrBayes (v.3.1.2; Huelsenbeck and Ronquist 2001). Parsimony analyses were conducted using the heuristic search algorithm with 500 random input orders and tree bisection–reconnection branch swapping. The reliability of the phylogenies identified by neighbor-joining and maximum parsimony was estimated using 500 replicates and one input order per replicate. In MrBayes, the Markov chain Monte Carlo search was run with four simultaneous chains for a total of 1,000,000 generations and sampled once every 100 generations. The amino acid substitution model was set to "mixed". Trees sampled prior to reaching convergence were discarded as "burn-in". Two independent runs were performed to ensure convergence in the Bayesian results. Posterior probabilities are presented from a 50% majority rule consensus of the remaining trees (n=4,786). GenBank accession and MIPS identifiers for sequences utilized in evolutionary analyses are included in Table 1.

Results

Type II S15a is an Evolutionarily Distinct Protein Found in Higher Plants

The *Arabidopsis* genome contains six genes that encode the r-protein S15a (Barakat et al. 2001). The deduced polypeptide sequences of four genes (S15aA, C, D, and F) share a high-percent identity to the rat ortholog (between 73.1% and 77.7%), whereas the deduced polypeptide sequences for the additional two genes (S15aB and E) show a much lower-percent identity to rat S15a (47.6% and 48.8%, respectively) (Chang et al. 2005). There is a high degree of conservation between the eukaryotic S15a and its prokaryotic ortholog S8, including the number of amino acids and molecular weight. To examine the relationship among *Arabidopsis* S15a proteins, Chang et al. (2005) utilized various evolutionary analyses. They concluded that the duplication event that led to the divergence of *Arabidopsis RPS15a* genes occurred prior to the divergence of moncots and eudicots. However, these analyses utilized relatively few eukaryotic S15a and organellar S8 sequences. Moreover, previous S15a phylogenies did not include representatives of algae, moss, or gymnosperms. To perform a more comprehensive analysis to examine the evolutionary relationship of Types I and II S15a and organellar S8 proteins, we searched publicly available databases for S15a- and S8-like sequences focusing primarily on genomes that have been completely sequenced. Pairwise, uncorrected distances were calculated between representative S15a and organellar S8 proteins (Table 2). The evolutionary distance within each group (Type I to Type I, Type II to Type II and chloroplast S8 to chloroplast S8) were substantially less than between-group distances. We identified mitochondrial S8 sequences for a diverse set of eukaryotes including green and brown algae, protozoans, fungi, liverwort, and moss (data not shown). However, many of these sequences were not utilized in the

Table 2 Divergence between S15a and S8 r-proteins of various species

Uncorrected distances given in top matrix, total residue difference in bottom matrix

		Type I S15a			Type II S15a			Chloroplast S8			Mitochondrial S8		
		Rno	Ath	Psi	Ath	Psi	Osa	Ath	Pab	Cat	Sce	Ota	Cat
Type I	Rno		0.22	0.23	0.54	0.56	0.550	0.78	0.794	0.810	0.859	0.765	0.756
	Ath	29		0.09	0.47	0.5	0.496	0.79	0.817	0.810	0.859	0.765	0.765
	Psi	30	11		0.51	0.52	0.519	0.78	0.810	0.817	0.859	0.782	0.748
Type II	Ath	69	61	66		0.33	0.225	0.78	0.786	0.770	0.859	0.82	0.815
	Psi	72	65	67	43		0.256	0.82	0.810	0.793	0.883	0.824	0.765
	Osa	71	64	67	29	33		0.79	0.810	0.794	0.875	0.849	0.815
cp S8	Ath	98	99	98	98	103	100		0.356	0.485	0.766	0.71	0.675
	Pab	100	103	102	99	102	102	47		0.462	0.766	0.73	0.700
	Cat	102	102	103	97	100	100	64	61		0.760	0.69	0.675
mt S8	Sce	110	110	110	110	113	112	98	98	98		0.73	0.718
	Ota	91	91	93	98	98	101	86	88	84	90		0.618
	Cat	90	91	89	97	91	97	81	84	81	89	76	

Ath Arabidopsis thaliana, *Cat Cholorkybus atmophyticus*, *Osa Oryza sativa*, *Ota Ostreococcus tauri*, *Pab Picea abies*, *Psi Picea sitchensis*, *Sce Saccharomyces cerevisiae*, *Rno Rattus norvegicus*

analyses presented here because, in preliminary analyses (not shown), these sequences did not fall into well-resolved clades suggesting that the sequences were extremely diverse. As highlighted in Table 2, the mitchondrial S8-like sequences utilized were quite distinct from one another. Notably, mitochondrial S8 within-group distances were similar to between-group distances indicating strong sequence divergence between S8 sequences of this organelle. Phylogenetic analysis was performed using three different tree-building methods (maximum parsimony, neighbor-joining, and Bayesian) employing *E. coli* S8 as the out group. All three methods evaluating eukaryotic S15a and eubacterial, archaeal, and oraganellar S8 amino acid sequences resolved five clades corresponding to chloroplast S8, mitochondrial S8, archaeal S8, Type I S15a, and Type II S15a (Fig. 2a). Plant Type I S15a sequences group with S15a sequences that are present in other eukaryotes including rat, *S. cerevesiae* and *Drosophila*, whereas the strongly supported clade with Type II S15a sequences is limited to plant-specific taxa. Interestingly, sequences from the green alga *Chlamydomonas reinhardtii* and the moss *Physcomitrella pattens*, are found in the Type I clade, whereas they are absent from the Type II clade (Fig. 2a). Given that the *C. reinhardtii* and the *P. patens* genomes have been fully sequenced (Merchant et al. 2007; Rensing et al. 2008) and that the Type II clade includes a gymnosperm (Sitka spruce, *Picea sitchensis*), this analysis supports the conclusion that the Type II S15a proteins are plant specific and further shows that the duplication event that led to the Type II S15a genes occurred after the divergence of Bryophytes but prior to the divergence of Spermatophytes. Of further interest is the placement of S15a sequences corresponding to the spikemoss, *Selaginella moellendorfii*. In all three of the analyses, there is strong

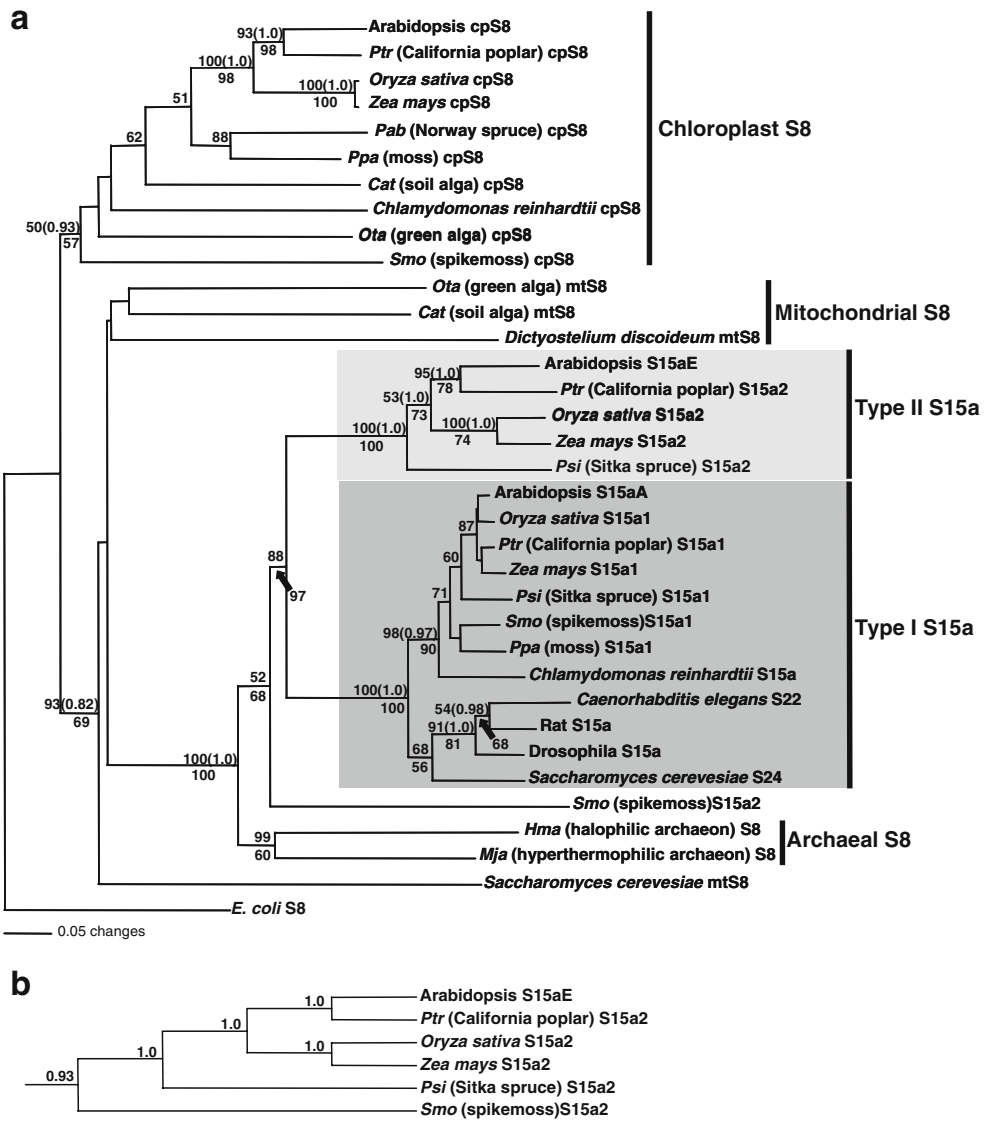

Fig. 2 Phylogenetic analysis of S8 and S15a r-proteins. **a** A phylogenetic tree was generated by the neighbor-joining method using uncorrected distances in PAUP version 4.0b10 (PPC) based on the amino acid sequences of eukaryotic S15a and mitochondrial, chloroplast, and prokaryotic S8 r-proteins. Bootstrap values from 500 replicates are indicated. Parsimony bootstrap values for clades supported above the 50% level are indicated below branches, whereas neighbor-joining bootstrap values based on uncorrected distances are indicated above the branches. Posterior probabilities based on a Bayesian analysis are listed above the branches in parenthesis. **b** A majority rule consensus tree was generated based on a Bayesian analysis in MrBayes and visualized in PAUP. Posterior probabilities are listed above the branches. Abbreviations: *Cat Chlorokybus atmophyticus*, *Hma Haloarcula marismortui*, *Mja Methanococcus jannaschii*, *Ota Ostreococcus tauri*, *Pab Picea abies*, *Ppa Physcomitrella patens*, *Psi Picea sitchensis*, *Ptr Populus trichocarpa*, *Smo Selaginella moellendorfii*

support for the Type I clade containing a *S. moellendorfii* sequence (Fig. 2a), whereas the placement of a distinct form of S15a in *S. moellendorfii* within the Type II clade is supported by the Bayesian analysis alone (Fig. 2b).

Structure and Organization of Type II S15a Genes

Analysis of gene structure indicates that the Type II S15a genes, *RPS15aB* and *RPS15aE* both contain three exons and two introns (Fig. 1). Overall, exon and intron size and location are well conserved between the two genes. Subtle exceptions include the length of the open reading frame of exon 1 (127 and 130 base pairs [bp] in *RPS15aB* and *RPS15aE*, respectively), the length of both introns (575 and 71 bp in *RPS15aB* and 477 and 77 bp in *RPS15aE*), and the length of the open reading frame in exon 3 (102 and 99 bp in *RPS15aB* and *RPS15aE*, respectively; Fig. 1). An alignment of expressed sequence tags (ESTs) available in GenBank for both genes (data not shown) suggests that the putative transcription start site is different for both genes (putative length of *RPS15aB* 5′ untranslated region is 40 bases, whereas the putative length of *RPS15aE* 5′ untranslated region is 81 bases). The 3′ untranslated regions of both genes varied considerably among the ESTs aligned (between five to 168 bases for *RPS15aB* and 39–310 bases for *RPS15aE*).

Genes Encoding Type II S15a are Differentially Expressed

Genomic-level studies of *Arabidopsis* r-protein gene family members confirmed that these genes are differentially expressed (Barakat et al. 2001). The four genes encoding Type I S15a in *Arabidopsis* were shown to be differentially expressed in various tissues and in response to various hormone treatments, temperature stress, and wounding (Hulm et al. 2005). In the case of the Type II S15a genes, Chang et al. (2005) found ESTs were reported for S15aB but not for S15aE; however, they also demonstrated that the S15aE protein is incorporated into ribosomes obtained by differential centrifugation from cultured *Arabidopsis* cells. To determine if the individual Type II S15a protein genes are differentially expressed in *Arabidopsis*, total RNA isolated from various organs and developmental stages was subjected to RT-PCR with gene-specific primers designed to bind within the coding region of *RPS15aB* and *RPS15aE* (Fig. 1). The results indicate that both Type II *RPS15a* genes are expressed in the tissues examined; however, the relative transcript abundance of the transcripts varies for the two genes (Fig. 3). *RPS15aB* is relatively well expressed in floral buds, moderately expressed in stems, bracts, siliques, and flowers. By contrast, the accumulation of this mRNA is apparently lower in seedling roots and rosette leaves. *RPS15aE* is relatively well expressed in all

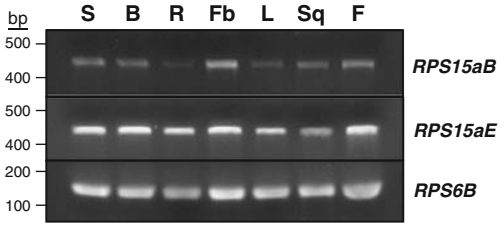

Fig. 3 RT-PCR analysis of Type II *RPS15a* gene expression patterns. S stems, *B* bracts, *R* roots, *Fb* floral buds, *L* leaves, *Sq* siliques, and *F* flowers were harvested as described in Materials and Methods. Expression of each Type II *RPS15a* gene was analyzed by RT-PCR using gene-specific primers. The expression level of an *RPS6B* gene was used as an internal loading control. The figure shown is representative of three biological replicates

of the tissues examined. Furthermore, the patterns of gene expression observed concurred with that found in the reference expression database Genevestigator (Hruz et al. 2008). Our results indicate that the two genes that encode Type II S15a are differentially expressed in the tissues examined.

Genetic Analysis of Disruption of Individual Type II S15a Genes

As indicated, in *Arabidopsis*, Type II S15a is encoded by the two genes *RPS15aB* and *RPS15aE* (Barakat et al. 2001). Multiple copies of a gene may result in functional redundancy, but there are examples in *Arabidopsis* where duplicated r-protein genes have been shown to be nonredundant (Van Lijsebettens et al. 1994; Williams and Sussex 1995; Ito et al. 2000; Degenhardt and Bonham-Smith 2008a). Therefore, it was of interest to examine the effect of disruption of individual members of the Type II S15a gene family. To that end, we utilized a reverse genetics approach with T-DNA insertion lines obtained from the *Arabidopsis* Biological Resource Center (ABRC) for *RPS15aB* and *RPS15aE* (Salk_074808 and Salk_118515, respectively; Alonso et al. 2003) and designated the insertion alleles, *rps15aB-mut1* and *rps15aE-mut1*. Genotypes of *rps15aB-mut1* and *rps15aE-mut1* mutant lines were characterized by genomic PCR with gene-specific primers and a T-DNA left-border primer (Figs. 1 and 4a). The T-DNA insertion sites of *rps15aB-mut1* and *rps15aE-mut1* were determined by sequencing (Fig. 1). The site of insertion in *rps15aB-mut1* is 103 bp upstream of the ATG translation start site. This differs from the exon 1 location predicted in SIGnAL (http://signal.salk.edu/). The T-DNA insertion for *rps15aE-mut1* is within the first intron, 556 bp downstream of the initiation codon, as predicted by SIGnAL. RT-PCR analyses of homozygous *rps15aB-mut1* and *rps15aE-mut1* seedlings confirmed that *RPS15aB* mRNA accumulation was not affected by the

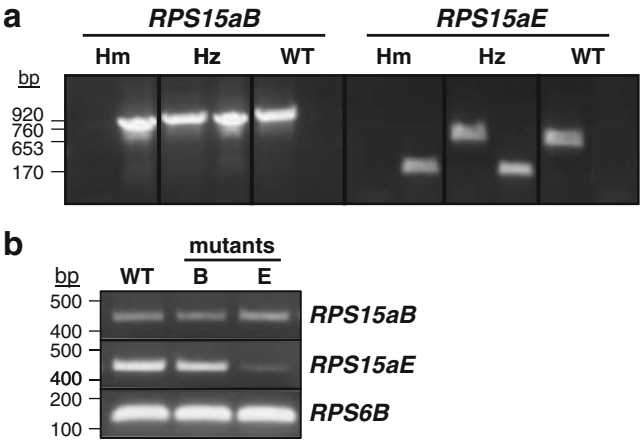

Fig. 4 Molecular characterization of Type II S15a T-DNA insertion lines. **a** Genotype determination for *rps15aB-mut1* and *rps15aE-mut1*. Genotypes were determined using primer pairs designed to flank the T-DNA insertion to identify WT plants, whereas gene-specific primers and a primer designed to bind to the left border of the T-DNA insert identified plants heterozygous (*Hz*) or homozygous (*Hm*) for the insert. Size of PCR products indicated in kilobase pairs. **b** Examination of Type II S15a transcript in *rps15aB-mut1* and *rps15aE-mut1* plants. RT-PCR was performed on 10-d-old *rps15aB-mut1*, *rps15aE-mut1*, and WT seedlings as described in Materials and Methods. The expression level the *RPS6B* gene was used as an internal loading control

T-DNA insertion in *rps15aB-mut1*, whereas *RPS15aE* mRNA accumulation was dramatically reduced in *rps15aE-mut1* confirming a gene knockdown mutation (Fig. 4b). Interestingly, the relative abundance of the *RPS15aB* transcript appeared to be unaltered in *rps15aE-mut1* seedlings.

To examine the effect of the knockdown in *RPS15aE* expression, we monitored the growth and development of *rps15aE-mut1* in phenotypic analyses as outlined by Boyes et al. (2001). Briefly, we examined the number of days plants took to reach specific developmental stages, leaf area, and radii at 10-, 12-, 14-leaf, and first-flower stages and total seed mass. There was no statistically significant difference between *rps15aE-mut1* knockdown and WT plants for the time to reach a developmental stage (Fig. 5a) or for seed mass (Fig. 5b). In addition, upon examination of leaf radii and areas, there was no statistically significant difference between *rps15aE-mut1* and WT at the various developmental stages examined with the exception of leaf area at the 12-leaf stage (Fig. 5c–e, $p<0.05$). By contrast, the general effect term showed that there is a highly significant difference between the mean radii and areas of *rps15aE-mut1* compared with WT (Fig. 5c–e; radii, $p<0.001$; area, $p<0.01$). Lastly, given that the Type II *RPS15a* gene family exhibits differential gene expression, particularly in seedling roots (Fig. 3), provided us the opportunity to examine the phenotypic effect of reduced expression of this entire gene family. Therefore, we

Fig. 5 Phenotypic characterization of *rps15aE-mut1* plants. **a** The number of days required to reach various key developmental stages (as outlined by Boyes et al. 2001) was determined for WT and *rps15aE-mut1* plants. **b** Seed mass at the end of the life cycle. **c**, **d** Leaf measurements. Leaf radius (**c**) and leaf area (**d**) of the largest leaf was measured at the 10-, 12-, 14-leaf, and 1st flower stages. Differences between WT and *rps15aE-mut1* in panels **a**–**d** were analyzed with a paired *t* test, and significant differences are indicated by **a**, **b** ($p< 0.05$). The *last set of bars* in panels **c** and **d** represent the treatment effect as determined by a two-way ANOVA. Significant differences of $p<0.01$ and $p<0.001$ are indicated by *asterisks* (** and ***, respectively). **e** Rosettes representative of WT and *rps15aE-mut1* phenotypes at the 10-, 12- and 14-leaf stages. *Bar*=1.4 cm. For all graphs, data represent the mean±SE ($n=15$); *white bars* indicate WT; *gray bars* indicate *rps15aE-mut1*

examined root growth in *rps15aE-mut1* compared with WT. *rps15aE-mut1* seedling roots are longer than WT seedling roots ($p<0.001$), yet appear to be thinner than those of the WT (Fig. 6a, b).

Greater mean rosette radii and leaf areas of *rps15aE-mut1* plants compared with WT may be due to alterations in cell size; therefore, we examined the leaves histologically at two developmental time points (when plants reached the 14-leaf stage [~4 weeks postimbibition] and 6 weeks postimbibition (Fig. 7a, b). The subepidermal palisade cells of the first leaf were significantly larger in *rps15aE-mut1* than in the WT at both developmental time points examined suggesting that the difference in rosette radii and area result from *rps15aE-mut1* plants possessing larger cells (14-leaf stage, $p<0.0001$; 6-week postimbibition, $p<0.01$; Fig. 7a–c). Interestingly, there is a more notable difference in cell size at the 14-leaf stage compared with 6 weeks postimbibition. Given an extended period of time, the response in *rps15aE-mut1* is reduced or diminished such that the difference in cell size between *rps15aE-mut1* and WT is less.

Discussion

Type II S15a is an Evolutionarily Distinct Protein Found in Seeded Plants

Our analyses have demonstrated that the Type II S15a protein is evolutionarily distinct and plant specific. Presence of sequences from the green alga *C. reinhardtii* and the moss *P. pattens* (which have fully sequenced genomes; Merchant et al. 2007; Rensing et al. 2008) in the Type I clade and absence of these species from the Type II clade (Fig. 2a) indicates that the duplication event that gave rise to the Type II genes occurred after the divergence of Bryophytes. In addition, the Type II clade is comprised only of plant species including angiosperms (both monocot and eudicot) and a gymnosperm (Sitka spruce, *P. sitchensis*) indicating that the Type II S15a proteins are plant specific

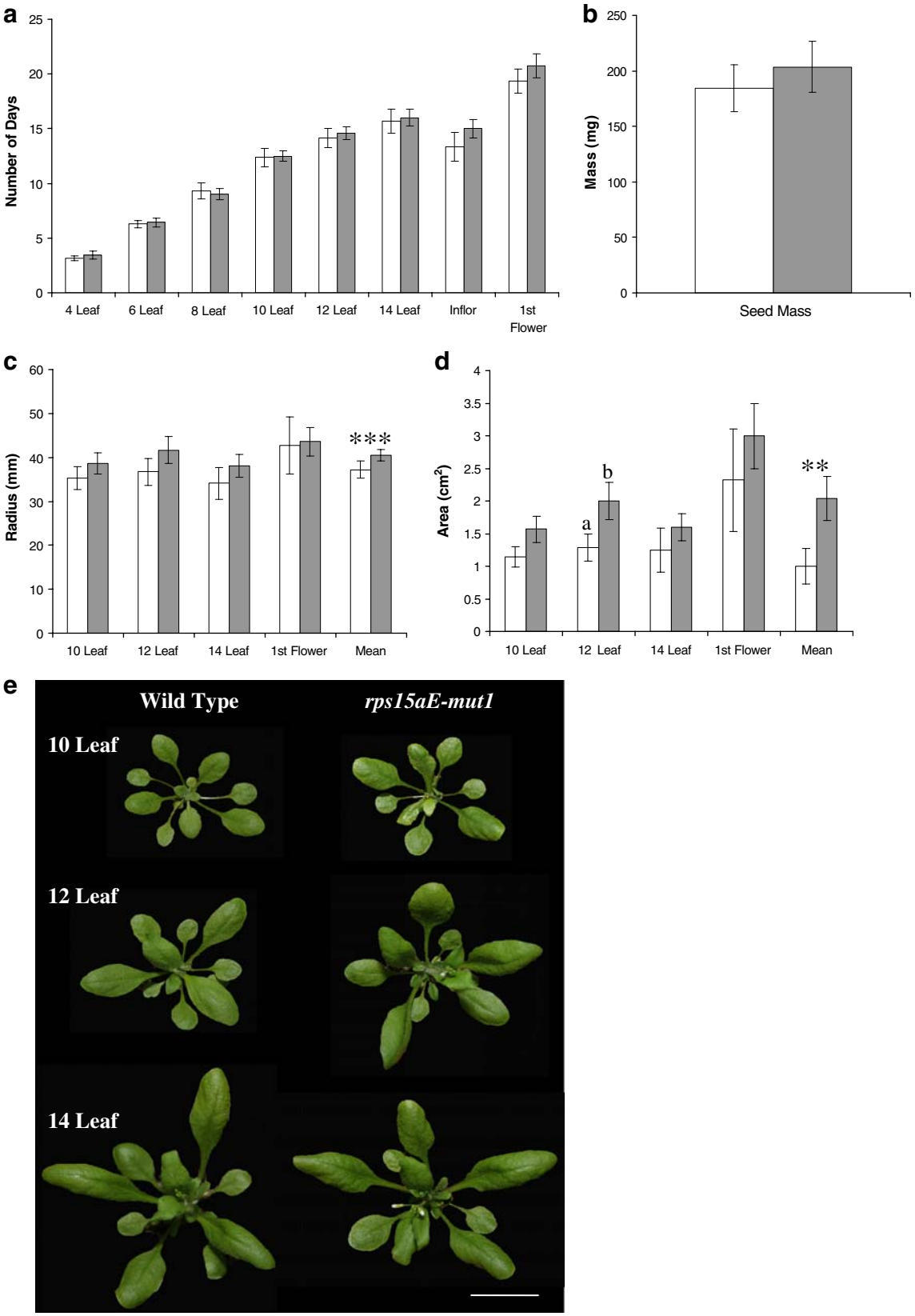
a
Number of Days
25
20
15
10
5
0
4 Leaf
6 Leaf
8 Leaf
10 Leaf
12 Leaf
14 Leaf
Inflor
1st Flower
b
Mass (mg)
250
200
150
100
50
0
Seed Mass
c
Radius (mm)
60
50
40
30
20
10
0
***
10 Leaf
12 Leaf
14 Leaf
1st Flower
Mean
d
Area (cm²)
4
3.5
3
2.5
2
1.5
1
0.5
0
a
b
**
10 Leaf
12 Leaf
14 Leaf
1st Flower
Mean
e
Wild Type
rps15aE-mut1
10 Leaf
12 Leaf
14 Leaf

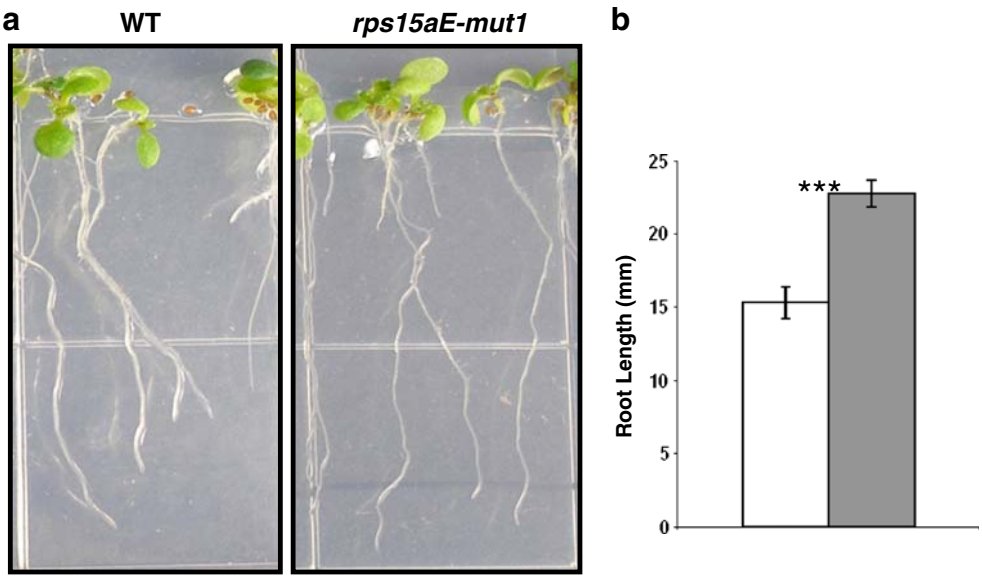

Fig. 6 Comparison of root length between WT and *rps15aE-mut1*. **a** WT and *rps15aE-mut1* seedlings were grown on MS containing plates for 22 d postimbibition. Root lengths were visualized under a stereoscopic microscope. **b** Individual roots were measured and analyzed with a two-sample *t* test. The data represent the mean±SE (WT, $n=20$; *rps15aE-mut1*, $n=33$). Significant differences ($p<0.001$) are indicated by *asterisks*. *White bars* indicate WT; *gray bars* indicate *rps15aE-mut1*

and that the duplication event that led to the Type II S15a genes occurred prior to the divergence seeded plants. Interestingly, spikemoss (*S. moellendorfii*), which is a member of the tracheophyte subdivision of the Kingdom Plantae representing the oldest extant vascular plant division, also possesses a form of S15a that is distinct from the Types I and II classification shown in Fig. 2a; however, with the Bayesian analysis, which incorporates probabilistic models of amino acid substitution, this distinct form groups within the Type II clade (Fig. 1b). Regardless of its exact position in the phylogenetic trees presented here, the analyses suggest that there may have been some sort of selective pressure such as loss of the mitochondrial S8 gene within the vascular plant lineage for the evolution of a novel form of ribosomal protein S15a.

Subcellular Location of Type II S15a

The previous findings of Adams et al. (2002), Chang et al. (2005), and Carroll et al. (2008) lead to the question: Is

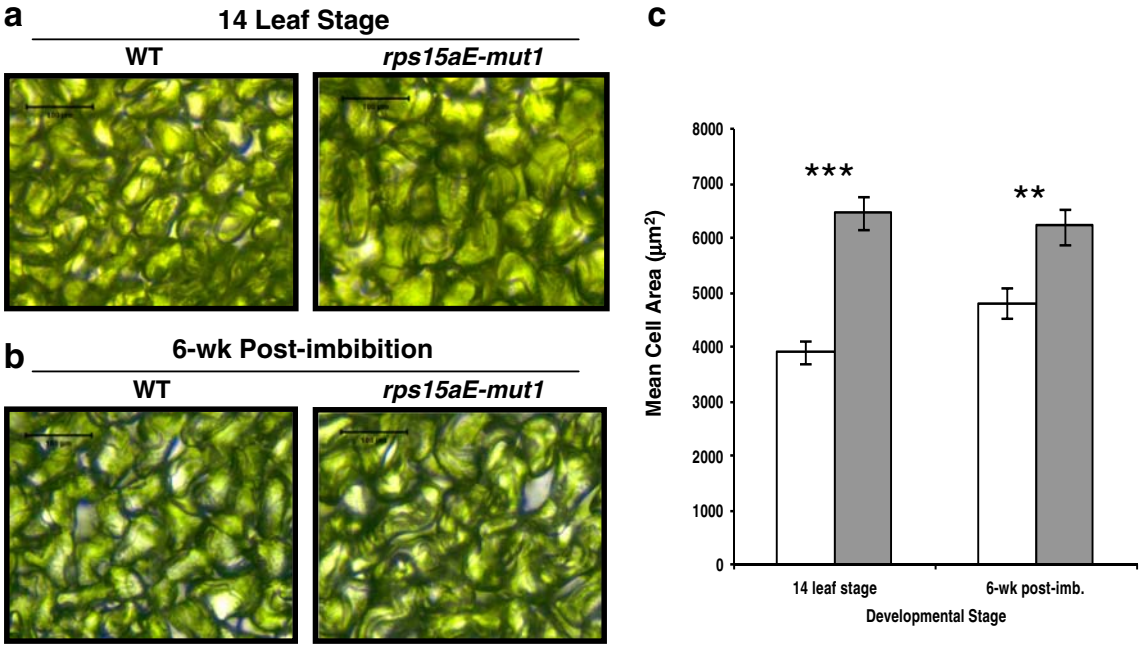

Fig. 7 Comparison of cell size between WT and *rps15aE-mut1*. Palisade cells in the subepidermal layer at the 14-leaf stage (**a**) or 6 weeks postimbibition were visualized by a light microscope (**b**) in WT and *rps15aE-mut1*. **c** Differences in mean cell size between WT and *rps15aE-mut1* were analyzed with a paired *t* test. Significant differences of $p<0.01$ and $p<0.001$ are indicated by *asterisks* (** and ***, respectively). (14-leaf stage, $n=16$; 6 weeks postimbibtion, $n=22$). *White bars* indicate WT; *gray bars* indicate *rps15aE-mut1*

Type II S15a found in both mitochondrial and cytosolic ribosomes? A comprehensive proteomic analysis of mitochondrial ribosomes from plants would be beneficial to elucidate the exact subcellular localization of the Type II S15a proteins. To date, analyses of the *Arabidopsis* mitochondrial proteome have only identified five mitochondrial r-proteins (S4, L3, L7/L12, L22, and L25) (Heazlewood et al. 2004; Heazlewood and Millar 2005). An approach that may unambiguously answer this question would be to epitope tag S15a proteins (Types I and II) in a manner that facilitated immunoprecipitation of the ribosome complex as shown for cytosolic RPL18 and RPL23 (Zanetti et al. 2005). The coimmunoprecipitated proteins could then be subsequently analyzed by mass spectrometry to determine the coassociated proteins.

Mitochondrial Ribosomes

It is well established that ribosomes of an archaebacterial ancestor gave rise to the cytosolic ribosomes of eukaryotes (Wittmann-Leibold et al. 1990; Matheson et al. 1990; Wool et al. 1995). By contrast, the r-proteins of plastids and mitochondria show strong evolutionary similarity to those of eubacteria and include organelle-specific proteins (Yamaguchi et al. 2000; Yamaguchi and Subramanian 2000; Graack and Wittmann-Liebold 1998; Koc et al. 2000; Koc et al. 2001). To examine the possibility that the Type II S15a sequences may correspond to mitochondrial r-protein S8, Chang et al. (2005) searched the GenBank database for S8/S15a sequences. This search resulted in numerous eukaryotic S15a and prokaryotic S8 sequences, several chloroplast S8, and few mitochondrial S8 sequences. The authors found that the mitochondrial S8-like sequences were quite divergent from one another. Similarly, our expanded homology search for S8/S15a sequences resulted in mitochondrial S8 sequences for a diverse set of eukaryotes including green and brown algae, protozoans, fungi, liverwort, and moss. Our analyses also indicate that the mitochondrial S8 sequences are quite divergent from one another. Distance values between mitochondrial S8 sequences (Table 2, Sce/Ota 0.726, Sce/Cat 0.718, and Ota/Cat 0.618) are similar to chloroplast S8/mitochondrial S8 distances (Ath cpS8/Ota mt S8 0.711, Ath cpS8/Cat mtS8 0.675, and Cat mtS8/Cat cpS8 0.675). Also, our homology search failed to identify mitochondrial S8 from higher eukaryotes. This concurs with other studies as a homology search of the *D. melanogaster* genome indicates that there is no mitochondrial S8 (Marygold et al. 2007) and mass spectrometric analysis of the mammalian mitochondrial 30S subunit failed to identify an S8 homologue (Koc et al. 2001).

Eubacterial-like mitochondrial S8 is apparently missing from higher eukaryotes (including higher plants) suggesting that this gene was lost sometime during the evolution of eukaryotes (perhaps more than once). If Type II S15a does in fact replace mitochondrial S8 in higher plants, then there is most likely an important role for Type II S15a in the evolution of seeded plants and perhaps in vascular plants in general (due to the second distinct form of S15a found in spikemoss). This led us to probe the functional significance of Type II S15a proteins using a forward genetics approach.

Genes Encoding Type II S15a are Differentially Expressed

The sequence similarity between the two *Arabidopsis* RPS15a Type II genes is high; yet, by use of gene-specific primers, we confirmed that the two genes display different expression patterns in *Arabidopsis* organs at different developmental stages. *RPS15aE* was constitutively expressed in the tissues/developmental stages we examined, whereas the expression pattern of *RPS15aB* varied from tissue to tissue. To date, all detailed analyses of *Arabidopsis* r-protein genes have illustrated distinctions in regulation of expression of gene family members (Larkin et al. 1989; Van Lijsebettens et al. 1994; Dresselhaus et al. 1999; Revenkova et al. 1999; Barakat et al. 2001; Hulm et al. 2005; McIntosh and Bonham-Smith 2005). For example, high levels of expression of one *Arabidopsis* L11 gene (*RPL11C*, previously called *RPL16B*) was observed in shoot and primary root meristems and lateral root primordia in response to auxin treatment, whereas expression of another L11 gene (*RPL11A*, previously called RPL16A) showed more cell-type specific gene expression (Williams and Sussex 1995). More recently, global studies of translational control have confirmed that r-protein mRNAs are highly regulated at the translational level (Branco-Price et al. 2005, 2008; Kawaguchi et al. 2004; Kawaguchi and Bailey-Serres 2005; Nicolaï et al. 2006). From these analyses, it appears that r-protein expression in plants may be regulated at the transcriptional and posttranscriptional levels.

Isoforms of Type II S15a may have distinct, nonoverlapping functions within the same cell, or different isoforms may fulfill identical functions within the cell but operate in distinct cell types, developmental periods, or in response to environmental conditions. An insertional mutation into *RPS15aE* resulted in reduced gene expression of *RPS15aE*, whereas *RPS15aB* levels were comparable to wild-type indicating that there was no upregulation of transcription of *RPS15aB* in response to a reduction in *RPS15aE* abundance. Similarly, Degenhardt and Bonham-Smith (2008b) found that loss of a single paralog (*RPL23aB*) in the two-member gene family encoding RPL23a did not result in upregulation of *RPL23aA*. Together, these results suggest that there is no

mechanism to compensate for the overall reduction for some r-protein transcripts.

Genetic Analysis of Disruption of Individual Type II S15a Genes

Our results demonstrate that the overall trend is for *rps15aE-mut1* plants to produce larger leaves, longer roots, and possess larger cells than WT plants as demonstrated in Figs. 5c–e, 6, and 7, respectively. Mutations in r-protein genes lead to abnormal growth and development such as the minute phenotype described for r-protein gene mutations in *Drosophila* (reviewed in Lambertsson 1998; Marygold et al. 2007). These mutations result in complications in growth and development that affect the entire organism due to reduced levels of protein synthesis (Marygold et al. 2007). In zebrafish, some r-protein gene mutations result in developmental defects with certain mutations resulting gene-specific phenotypes (Uechi et al. 2006). Additionally, there is increasing evidence for the role of r-proteins in plant development. Mutations in *Arabidopsis* S13 and S18 genes were shown to cause a pointed first leaf (pfl) phenotype remarkably indicating that mutations that alter the expression of r-protein genes may confer a similar phenotype (Van Lijsebettens et al. 1994; Ito et al. 2000). In *pfl1*, a T-DNA insertion into the S18A (*RPS18A*) gene resulted in complete loss-of-function mutation (Van Lijsebettens et al. 1994). Although S18 is encoded by three genes that appear to have overlapping expression, synthesis in mitotically active tissues seems to be required for normal leaf development. In *pfl2*, caused by a *Ds* insertion into the S13A (*RPS13B*) gene, a significantly reduced number and increased size of subepidermal palisade cells of the first leaf was observed (Ito et al. 2000). A semidominant mutation into the S5 gene (*RPS5A*) led to early embryonic developmental defects (Weijers et al. 2001). Yao et al. (2008) demonstrated that mutations into r-protein genes encoding L5, L24, and L28 resulted in abnormal leaf patterning, and recent analyses have demonstrated a role of r-proteins L5, L9, and L10a in the development of *Arabidopsis* via interactions with the Myb-domain transcription factor asymmetric leaves1 (Pinon et al. 2008). Finally, in *Arabidopsis*, the *HUELLENLOS* gene encodes mitochondrial ribosomal protein L14 which is essential for normal ovule development (Skinner et al. 2001).

Our data indicate that *rps15aE-mut1* plants are larger than the wild-type suggesting that this mutation is not likely to result in suboptimal levels of protein synthesis as seen with typical r-protein mutations. Similarly, in tobacco, a reduction in L3 levels resulted in a reduction in cell number yet an increase in cell size leading the authors to speculate that this protein is involved in regulating the cell cycle (Popescu and Tumer 2004). In addition, there is increasing evidence that deregulated protein synthesis plays an important role in human cancer (reviewed in Bilanges and Stokoe 2007). In zebrafish, heterozygous mutants for S15a resulted in a significant increase in tumor formation suggesting that this protein acts as a tumor suppressor (Amsterdam et al. 2004). Our data suggest that the S15aE isoform of Type II S15a may be acting to deregulate protein synthesis. Whether it is affecting cytosolic or mitochondrial translation remains to be determined.

Acknowledgments This work was supported, in part, by an intramural University Research Council grant awarded to Kathleen Szick-Miranda. Stacey Abidayo and Ammar S. Zanial were supported by the Student Research Scholars Program at CSUB and by the MARC U*STAR training program, award number T34GM069349, from the National Institute of General Medical Sciences. The content is solely the responsibility of the authors and does not necessarily represent the official views of the National Institute of General Medical Sciences or the National Institutes of Health. Ali S. Zanial was supported by the Student Research Scholars Program at CSUB. In addition, we are grateful to Brandon Pratt for statistical assistance and helpful discussions, Julia Bailey-Serres for critical review of this manuscript, Elizabeth Waters and Virginia Vandergon for their comments and discussion on the phylogenetic analyses, and Rick Miranda for experimental design.

References

Adams K, Daley D, Whelan J, Palmer J (2002) Genes for two mitochondrial ribosomal proteins in flowering plants are derived from their chloroplast of cytosolic counterparts. Plant Cell 14:931–943

Alonso J et al (2003) Genome-wide insertional mutagenesis of *Arabidopsis thaliana*. Science 301:653–657

Amsterdam A, Sadler KC, Lai K, Farrington S, Bronson RT, Lees JA, Hopkins N (2004) Many ribosomal protein genes are cancer genes in zebrafish. PLoS Biology 2(5):690–698

Barakat A, Szick-Miranda K, Chang I-F, Guyot R, Blanc G, Cooke R, Delseny M, Bailey-Serres J (2001) The organization of cytoplasmic ribosomal protein genes in the *Arabidopsis* genome. Plant Physiol 127(2):398–415

Bilanges B, Stokoe D (2007) Mechanisms of translational deregulation in human tumors and therapeutic intervention strategies. Oncogene 26:5973–5990

Boyes D, Zayed A, Ascenzi R, McCaskill A, Hoffman N, Davis K, Gorlach J (2001) Growth stage-based phenotypic analysis of *Arabidopsis*: a model for high throughput functional genomics in plants. Plant Cell 13:1499–1510

Branco-Price C, Kawaguchi R, Ferriera R, Bailey-Serres J (2005) Genome-wide analysis of transcript abundance and translation in *Arabidopsis* seedlings subjected to oxygen deprivation. Ann Bot 96:647–660

Branco-Price C, Hamersky KA, Jang CJH, Larive CK, Bailey-Serres J (2008) Selective mRNA translation coordinates energetic and metabolic adjustments to hypoxia and reoxygenation in *Arabidopsis thaliana*. Plant J 56(5):743–755

Brodersen DE, Clemons WM Jr, Carter AP, Wimberly BT, Ramakrishnan V (2002) Crystal structure of the 30S ribosomal subunit from *Thermus thermophilus*: structure of the proteins and their interactions with 16S RNA. J Mol Biol 316(3):725–768

Cammarano P, Pons S, Romeo A, Galdieri M, Gualerzi C (1972) Characterization of unfolded and compact ribosomal subunits from plants and their relationship to those of lower and higher animals: evidence for physicochemical heterogeneity among eucaryotic ribosomes. Biochim Biophys Acta 281(4):571–596

Carroll AJ, Heazlewood JL, Ito J, Millar AH (2008) Analysis of the *Arabidopsis* cytosolic ribosome proteome provides detailed insights into its components and their post-translational modification. Mol Cell Proteomics 7(2):347–369

Chandramouli P, Topf M, Menetret JF, Eswar N, Cannone JJ, Gutell RR, Sali A, Akey CW (2008) Structure of the mammalian 80S ribosome at 8.7Å resolution. Structure 16:535–548

Chang I-F, Szick-Miranda K, Pan S, Bailey-Serres J (2005) Proteomic characterization of evolutionarily conserved and variable proteins of *Arabidopsis* cytosolic ribosomes. Plant Physiol 137:848–862

Davies C, Ramakrishnan V, White SW (1996) Structural evidence for specific S8-RNA and S8-protein interactions within the 30S ribosomal subunit: ribosomal protein S8 from *Bacillus stearothermophilus* at 1.9Å resolution. Structure 4(9):1093–1104

Dean D, Yates JL, Nomura M (1981) *Escherichia coli* ribosomal protein S8 feedback regulates part of *spc* operon. Nature 289 (5793):89–91

Degenhardt RF, Bonham-Smith PC (2008a) *Arabidopsis* ribosomal proteins RPL23aA and RPL23aB are differentially targeted to the nucleolus and are disparately required for normal development. Plant Physiol 147:128–142

Degenhardt RF, Bonham-Smith PC (2008b) Transcript profiling demonstrates absence of dosage compensation in *Arabidopsis* following loss of a single *RPL23a* paralog. Planta 228:627–640

Dresselhaus T, Cordts S, Heuer S, Sauter M, Loerz H, Kranz E (1999) Novel ribosomal genes from maize are differentially expressed in the zygotic and somatic cell cycles. Mol Gen Genet 261(2):416–427

Giavalisco P, Wilson D, Kreitler T, Lehrach H, Klose J, Gobom J, Fucini P (2005) High heterogeneity within the ribosomal proteins of the *Arabidopsis thaliana* 80S ribosome. Plant Mol Biol 57:577–591

Graack HR, WittmannLiebold B (1998) Mitochondrial ribosomal proteins (MRPs) of yeast. Biochem J 329(PT3):433–448

Heazlewood J, Tonti-Filippini J, Gout A, Day D, Whelan J, Millar AH (2004) Experimental analysis of the *Arabidopsis* mitochondrial proteome highlights signaling and regulator components, provides assessment of targeting prediction programs and indicates plant-specific mitochondrial proteins. Plant Cell 16:241–256

Heazlewood JL, Millar AH (2005) *Arabidopsis* mitochondrial proteomics. Methods Mol Biol 372:559–571

Held WA, Ballou B, Mizushima S, Nomura M (1974) Assembly mapping of 30S ribosomal proteins from *Escherichia coli*. Further studies. J Biol Chem 249(10):3103–3111

Hershey JW (1991) Translational control in mammalian cells. Annu Rev Biochem 60(25):717–755

Hruz T, Laule O, Szabo G, Wessendorp F, Bleuler S, Oertle L, Widmayer P, GruissemW, Zimmermann P (2008) Genevestigator V3: a reference expression database for the meta-analysis of transcriptomes. Advances in Bioinformatics 2008, Article ID 420747. doi:10.1155/2008/420747

Huelsenbeck JP, Ronquist F (2001) MrBayes: Bayesian inference of phylogenetic trees. Bioinformatics 17(8):754–755

Hulm J, McIntosh K, Bonham-Smith P (2005) Variation in transcript abundance among the four members of the *Arabidopsis thaliana* ribosomal protein *s15a* gene family. Plant Sci 169:267–278

Ito T, Kim G-T, Shinozaki K (2000) Disruption of an *Arabidopsis* cytoplasmic ribosomal protein S13-homologous gene by transposon-mediated mutagenesis causes aberrant growth and development. Plant J 22(3):257–264

Kawaguchi R, Bailey-Serres J (2005) mRNA sequence features responsible for translational regulation in *Arabidopsis*. Nucleic Acids Res 33(3):955–965

Kawaguchi R, Girke T, Bray EA, Bailey-Serres J (2004) Differential mRNA translation contributes to gene regulation under non-stress and dehydration stress conditions in *Arabidopsis thaliana*. Plant J 38:823–839

Koc EC, Burkhart W, Blackburn K, Moseley A, Koc H, Spremulli LL (2000) A proteomics approach to the identification of mammalian mitochondrial small subunit ribosomal proteins. J Biol Chem 275(42):32585–32591

Koc EC, Burkhart W, Blackburn K, Moseley A, Spremulli LL (2001) The small subunit of the mammalian mitochondrial ribosome: identification of the full complement of ribosomal proteins present. J Biol Chem 276(22):19363–19374

Lambertsson A (1998) The minute genes in *Drosophila* and their molecular functions. Adv Genet 38:69–134

Larkin JC, Hunsperger JP, Culley D, Rubenstein I, Silflow CD (1989) The organization and expression of a maize ribosomal protein gene family. Genes Dev 3(4):500–509

Lavoie C, Tam R, Clark M, Lee H, Sonenberg N, Lasko P (1994) Suppression of a temperature-sensitive cdc33 mutation of yeast by a multicopy plasmid expressing a *Drosophila* ribosomal protein. J Biol Chem 269(20):14625–14630

Lee SW, Berger SJ, Martinovic S, Pasa-Tolic L, Andereson GA, Shen Y, Zhao R, Smith RD (2002) Direct mass spectrometric analysis of intact proteins of the yeast large ribosomal subunit using capillary LC/TFICR. Proc Natl Acad Sci USA 99:5942–5947

Louie DF, Resing KA, Lewis TS, Ahn NG (1996) Mass spectrometric analysis of 40S ribosomal proteins from rat-1 fibroblasts. J Biol Chem 271:28189–28198

McIntosh KB, Bonham-Smith PC (2005) The two ribosomal protein *L23A* genes are differentially transcribed in *Arabidopsis thaliana*. Genome 48:443–454

Manuell AL, Yamaguchi K, Haynes PA, Milligan RA, Mayfield SP (2005) Composition and structure of the 80S ribosome from the green alga *Chlamydomonas reinhardtii*: 80S ribosomes are conversed in plants and animals. J Mol Biol 351:266–279

Marygold SJ, Roote J, Reuter G, Lambertsson A, Ashburner M, Millburn GH, Harrison PM, Yu Z, Kenmochi N, Kaufman TC, Leevers SJ, Cook KR (2007) The ribosomal protein genes and minute loci of *Drosophila*. Genome Biol 8(10):R216. doi:10.1186/gb-2007-8-10-r216

Matheson AT, Auer J, Ramierez C, Bock A (1990) Structure and evolution of archaebacterial ribosomal proteins. In: Hill WE, Dahlberg A, Garrett RE, Moore PB, Schlessinger D, Warner DC (eds) The ribosome: structure, function and evolution. American Society of Microbiologists, Wasington, D.C, pp 617–633

Merchant SS et al (2007) The *Chlamydomonas* genome reveals the evolution of key animal and plant functions. Science 318 (5848):245–250

Merrick WC, Hershey JWB (1996) The pathway and mechanism of eukaryotic protein synthesis. In: Hershey JWB, Mathews MB, Sonenberg N (eds) Translational control. Cold Spring Harbor Laboratory, Cold Spring Harbor, pp 31–69

Murashige T, Skoog F (1962) A revised medium for rapid growth and bio-assays with tobacco tissue cultures. Physiol Plant 15(3):473–497

Nicolaï M, Roncato MA, Canoy AS, Rouquie D, Sarda X, Freyssinet G, Robaglia C (2006) Large-scale analysis of mRNA translation states during sucrose starvation in *Arabidopsis* cells identifies cell proliferation and chromatin structure as targets of translational control. Plant Physiol 141(2):663–673

Nygård O, Nilsson L (1990) Translational dynamics. Interactions between the translational factors, tRNA and ribosomes during eukaryotic protein synthesis. Eur J Biochem 191(1):1–17

Odintsova TI, Muller EC, Ivanov AV, Egorov TA, Bienert R, Vladimirov SN, Kostka S, Otto A, Wittmann-Liebold B, Karapova GG (2003) Characterization and analysis of posttranslational modifications of the human large cytoplasmic ribosomal

subunit proteins by mass spectrometry and Edman sequencing. J Protein Chem 22:249–258

Pinon V, Etchells JP, Rossignol P, Collier SA, Arroyo JM, Martienssen RA, Byrne ME (2008) Three PIGGYBACK genes that specifically influence leaf patterning encode ribosomal proteins. Development 135(7):1315–1324

Popescu SC, Tumer NE (2004) Silencing of ribosomal protein L3 genes in *N. tabacum* reveals coordinate expression and significant alterations in plant growth, development and ribosome biogenesis. Plant J 39:29–44

Proud CG (2007) Signalling to translation: how signal transduction pathways control the protein synthetic machinery. Biochem J 403:217–234

Rensing et al (2008) The *Physcomitrella* genome reveals evolutionary insights into the conquest of land by plants. Science 319 (5859):64–69

Revenkova E, Masson J, Koncz C, Afsar K, Jakovleva L, Paszkowski J (1999) Involvement of *Arabidopsis thaliana* ribosomal protein S27 in mRNA degradation triggered by genotoxic stress. EMBO J 18(2):490–499

Skinner DJ, Baker SC, Meister RJ, Broadhvest J, Schneitz K, Gasser CS (2001) The *Arabidopsis HUELLENLOS* gene, which is essential for normal ovule development, encodes a mitochondrial ribosomal protein. Plant Cell 13(12):2719–2730

Svensson P, Changchien LM, Craven GR, Noller HF (1988) Interaction of ribosomal proteins, S6, S8, S15 and S18 with the central domain of 16S ribosomal RNA. J Mol Biol 200(2):301–308

Spahn CM, Beckmann R, Eswar N, Penczek PA, Sali A, Blobel G, Frank J (2001) Structure of 80 S ribosome from *Saccharomyces cerevisiae*-tRNA-ribosome and subunit–subunit interactions. Cell 107:3733–3786

Spahn CM, Gomez-Lorenzo MG, Grassucci RA, Jorgensen R, Andersen GR, Bechmann R, Penczek PA, Ballesta JPG, Frank J (2004) Domain movements of elongation factor eEF2 and the eukaryotic 80S ribosome facilitate tRNA translocation. EMBO J 23:1008–1019

Tishchenko SV, Vassilieva JM, Platonova OB, Serganov AA, Fomenkova NP, Mudrik ES, Piendl W, Ehresmann C, Ehresmann B, Garber MB (2001) Isolation, crystallization, and investigation of ribosomal protein S8 complexed with specific fragments of rRNA of bacterial or archaeal origin. Biochemistry (Moscow) 66 (9):948–953

Thompson JD, Higgins DG, Gibson TJ (1994) CLUSTAL W: improving the sensitivity of progressive multiple sequence alignment through sequence weighting, position-specific gap penalties and weight matrix choice. Nucleic Acids Res 22 (22):4673–4680

Uechi T, Nakajima Y, Nakao A, Torihara H, Chakraborty A, Inoue K, Kenmochi N (2006) Ribosomal protein gene knockdown causes developmental defects in zebrafish. PLoS ONE 1:e37

Weijers D, Dijk MF, Vencken RJ, Quint A, Hooykaas P, Offringa R (2001) An *Arabidopsis* minute-like phenotype caused by a semi-dominant mutation in a *Ribosomal Protein S5* gene. Development 128:4289–4299

Williams ME, Sussex IM (1995) Developmental regulation of ribosomal protein L16 genes in *Arabidopsis thaliana*. Plant J 8 (1):65–76

Wittmann-Leibold B, Kopke AKE, Arndt E, Kromer W, Hatakeyama T, Wittmann H-G (1990) Sequence comparison and evolution of ribosomal proteins and their genes. In: Hill WE, Dahlberg A, Garrett RE, Moore PB, Schlessinger D, Warner DC (eds) The ribosome: structure, function and evolution. American Society of Microbiologists, Washington, D.C., pp 598–616

Wool IG, Chan Y-L, Gluck A (1995) Structure and evolution of mammalian ribosomal proteins. Biochem Cell Biol 73(11–12):933–947

Van Lijsebettens M, Vanderhaeghen R, De Block M, Bauw G, Villarroel R, Van Montagu M (1994) An S18 ribosomal protein gene copy at the *Arabidopsis* PFL locus affects plant development by its specific expression in meristems. EMBO J 13 (14):3378–3388

Verschoor A, Srivastava S, Grassucci R, Frank J (1996) Native 3D structure of eukaryotic 80S ribosome: morphological homology with *E. coli* 70S ribosome. J Cell Biol 133:495–505

Yamaguchi K, Subramanian AR (2000) The plastid ribosomal proteins - Identification of all the proteins in the 50S subunit of an organelle ribosome (chloroplast). J Biol Chem 275(37):28466–28482

Yamaguchi K, von Knoblauch K, Subramanian AR (2000) The plastid ribosomal proteins—identification of all the proteins in the 30S subunit of an organelle ribosome (chloroplast). J Biol Chem 275 (37):28455–28465

Yao Y, Ling Q, Wang H, Haung H (2008) Ribosomal proteins promote leaf adaxial identity. Development 135(7):1325–1334

Yu Y, Ji H, Doudna JA, Leary JA (2005) Mass spectrometric analysis of the human 40S ribosomal subunit: native and HCV IRES-bound complexes. Protein Sci 14:1438–1446

Zanetti ME, Chang IF, Gong F, Galbraith DW, Bailey-Serres J (2005) Immunopurification of polyribosomal complexes of *Arabidopsis* for global analysis of gene expression. Plant Physiol 138:624–635